Search for Spatially Extended *Fermi*-LAT Sources Using Two Years of Data

Joshua Lande,
Stefan Funk,
Markus Ackermann

February 15, 2012

Search for Spatially Extended *Fermi*-LAT Sources Using Two Years of Data

J. Lande[1,2], M. Ackermann[3,4], A. Allafort[1], J. Ballet[5], K. Bechtol[1], T. H. Burnett[6], J. Cohen-Tanugi[7], A. Drlica-Wagner[1], S. Funk[1,8], F. Giordano[9,10], M.-H. Grondin[11,12], M. Kerr[1], M. Lemoine-Goumard[13,14]

- Cat II paper
- Internal referees: Marianne Lemoine-Goumard + Johann Cohen-Tanugi (+ unofficially Jean Ballet)
- Submitted to ApJ

Section 2.1. Modeling Extended Sources in the pointlike Package

New method to study spatially-extended *Fermi*-LAT sources

- Description of `pointlike`
- Implementation of extended sources
- Simultaneously Fit position + extension
- speed up likelihood computation
- Cross check TS + spectral values using `gtlike`

Fig. 2: LAT PSF

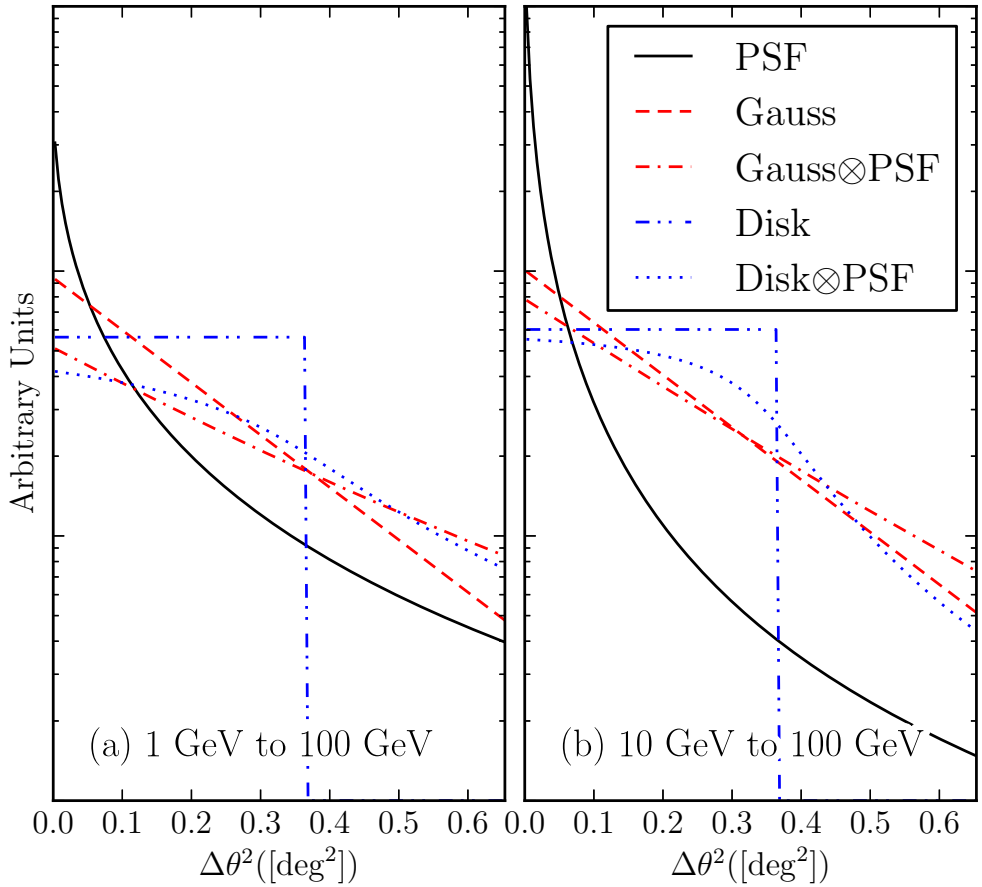
PSF
Gauss
Gauss⊗PSF
Disk
Disk⊗PSF
Arbitrary Units
(a) 1 GeV to 100 GeV
(b) 10 GeV to 100 GeV
0.0 0.1 0.2 0.3 0.4 0.5 0.6
$\Delta\theta^2([\mathrm{deg}^2])$

Table 1: False-Detection Rate

Table 1. Monte Carlo Spectral Parameters

Spectral Index	Flux[a] ($\mathrm{ph\,cm^{-2}\,s^{-1}}$)	$N_{1-100\mathrm{GeV}}$	$\langle \mathrm{TS} \rangle_{1-100\mathrm{GeV}}$	$N_{10-100\mathrm{GeV}}$	$\langle \mathrm{TS} \rangle_{10-100\mathrm{GeV}}$
1.5	3×10^{-7}	18938	22233	18938	8084
	10^{-7}	19079	5827	19079	2258
	3×10^{-8}	19303	1276	19303	541
	10^{-8}	19385	303	19381	142
	3×10^{-9}	18694	62	12442	43
2	10^{-6}	18760	22101	18760	3033
	3×10^{-7}	18775	4913	18775	730
	10^{-7}	18804	1170	18803	192
	3×10^{-8}	18836	224	15256	50
	10^{-8}	17060	50	...	...
2.5	3×10^{-6}	18597	19036	18597	786
	10^{-6}	18609	4738	18608	208
	3×10^{-7}	18613	954	15958	53
	10^{-7}	18658	203	...	...
	3×10^{-8}	14072	41	...	...
3	10^{-5}	18354	19466	18354	215
	3×10^{-6}	18381	4205	15973	54
	10^{-6}	18449	966	...	...
	3×10^{-7}	18517	174	...	...
	10^{-7}	13714	41	...	...

[a]Integral 100 MeV to 100 GeV flux.

- Simulate point-like sources
- Test for extension
- Good agreement with Wilk's Theorem
- Use $\sqrt{\mathrm{TS}_{\mathrm{ext}}}$ as a measure of significance
- $\sim 20,000$ Simulations per spectral model!
- Test in 1 GeV to 100 GeV + 10 GeV to 100 GeV energy range

Fig. 3+4: False-Detection Rate (cont)

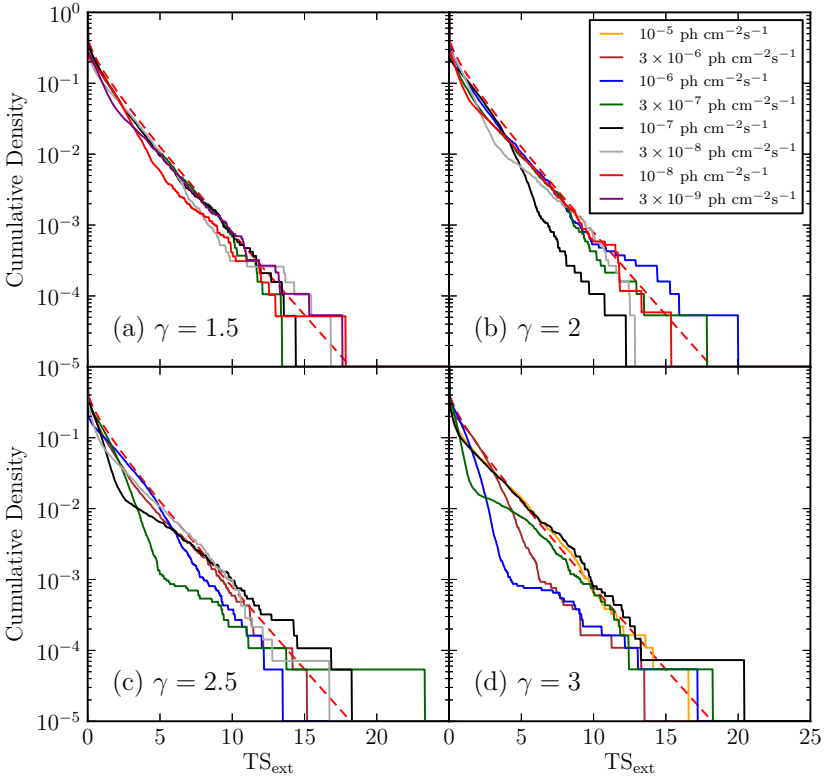

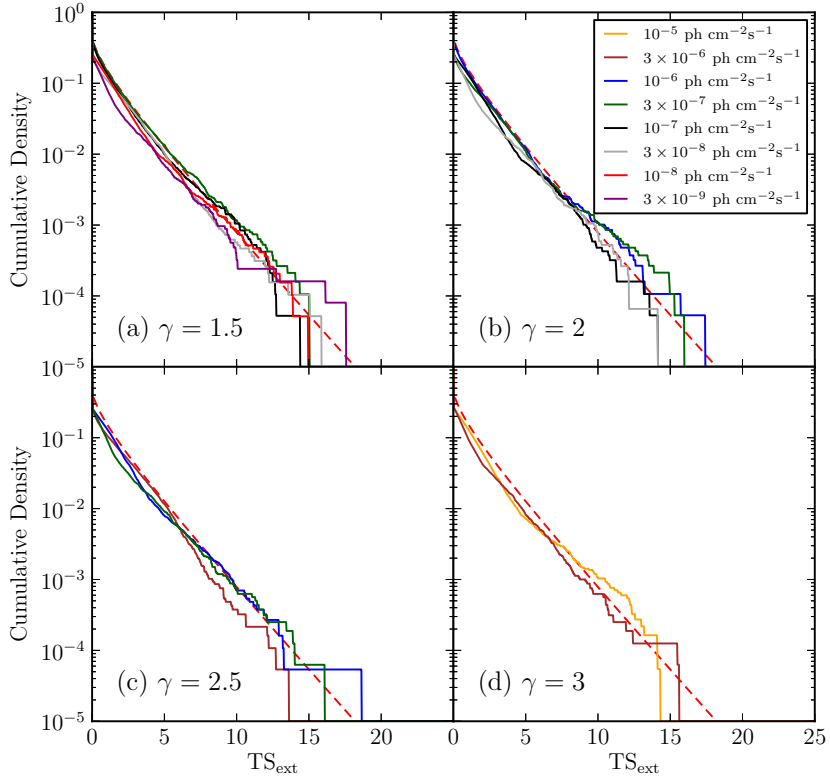

Fig. 5: Detection Threshold

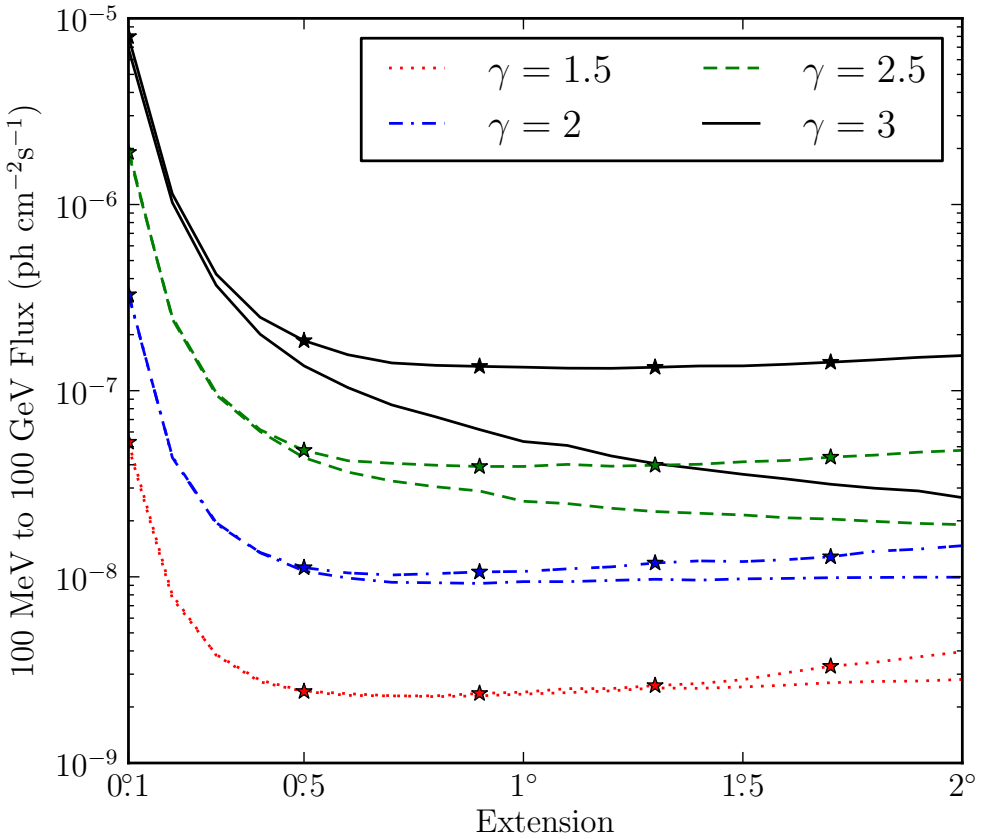

- Detetion threshold to extension
- $\langle \mathrm{TS}_{\mathrm{ext}} \rangle = 16$
- Vary spectra, background, energy range
- Overlay extended sources
- Reference for future publications!

Fig. 6: Detection Threshold (cont)

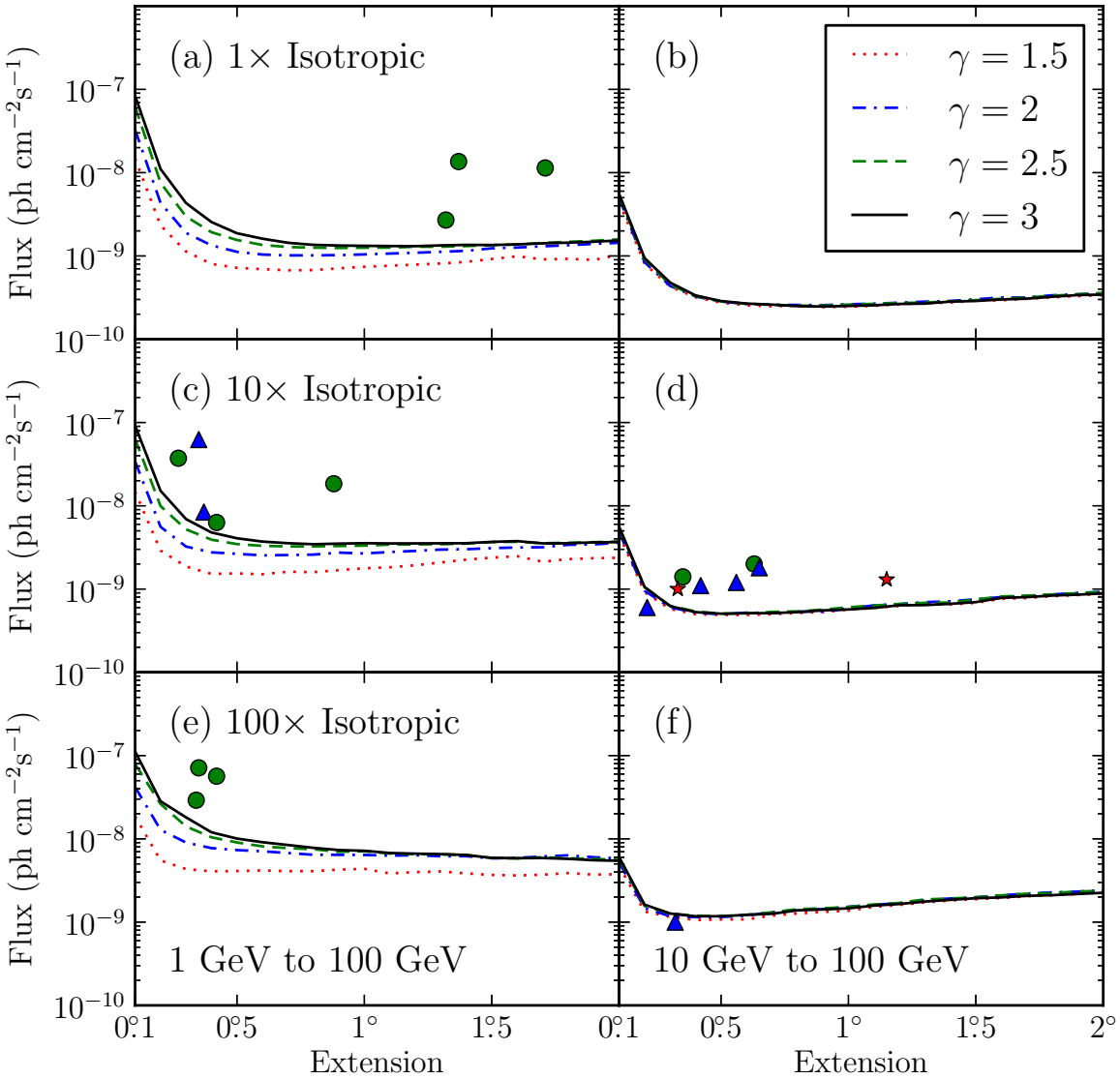

- Compute sensitivty for different background levels, energy ranges.

Table 2: Detection Threshold (cont)

Table 2. Extension Detection Threshold

γ	BG	0.1	0.2	0.3	0.4	0.5	0.6	0.7	0.8	0.9	1.0	1.1	1.2	1.3	1.4	1.5	1.6	1.7	1.8	1.9	2.0
E>1 GeV																					
1.5	1×	148.1	23.3	11.3	8.0	7.2	6.9	6.7	6.8	7.1	7.4	7.6	7.9	8.1	8.5	9.2	9.9	9.1	9.2	9.0	10.3
	10×	148.4	29.0	18.7	15.2	15.4	15.0	16.1	16.0	16.8	17.7	18.2	19.3	20.9	22.5	23.8	24.8	21.3	22.8	23.4	23.7
	100×	186.8	55.0	43.4	40.7	41.0	41.8	40.9	40.9	42.7	43.6	38.4	39.9	40.6	38.4	36.9	36.3	37.1	38.8	37.2	37.6
2	1×	328.4	43.4	18.9	13.4	11.2	10.4	10.2	10.2	10.2	10.4	10.7	10.9	11.2	11.5	12.4	12.6	13.0	13.4	14.0	14.4
	10×	341.0	55.9	32.3	27.6	26.5	25.4	25.6	25.9	27.4	26.8	27.8	28.7	29.8	30.1	31.0	31.5	31.7	34.0	34.3	35.9
	100×	420.5	128.3	90.2	77.3	73.3	70.8	67.5	64.3	64.2	64.1	62.8	63.6	61.7	61.9	58.4	59.0	61.4	63.3	60.1	58.1
2.5	1×	627.1	75.6	29.8	19.3	15.5	13.5	12.8	12.6	12.5	12.5	12.6	12.9	12.9	13.1	13.5	13.7	14.3	14.8	15.2	15.8
	10×	638.9	99.1	52.1	39.1	34.6	33.0	32.5	32.5	32.8	33.2	34.1	34.3	34.5	35.1	36.6	36.9	35.5	36.0	36.5	37.3
	100×	795.0	262.1	140.9	104.3	90.4	81.2	77.2	75.1	69.7	70.9	66.5	65.6	64.9	64.0	58.9	58.1	60.2	58.4	57.5	55.8
3	1×	841.5	110.6	43.2	25.5	18.7	16.1	14.4	13.6	13.3	13.2	13.1	13.1	13.4	13.6	13.5	13.8	14.2	14.4	14.8	15.4
	10×	921.6	151.3	69.1	47.8	40.7	37.1	35.5	34.5	35.1	35.5	35.3	35.3	35.4	35.5	36.8	37.6	35.3	35.4	36.3	36.6
	100×	1124.1	282.9	181.1	119.8	100.7	91.1	84.3	77.9	73.3	71.8	67.6	66.4	65.5	63.9	59.0	58.6	58.8	57.5	55.4	54.4
E>10 GeV																					
1.5	1×	44.6	8.0	4.3	3.2	2.7	2.6	2.5	2.5	2.4	2.5	2.5	2.6	2.7	2.8	2.9	2.9	3.1	3.2	3.3	3.4
	10×	45.2	9.2	5.8	5.0	4.9	4.9	5.0	5.2	5.3	5.7	5.9	6.3	6.6	6.5	6.8	7.6	7.8	8.2	8.5	8.7
	100×	47.3	13.4	11.6	10.6	10.8	10.8	12.0	12.7	13.2	13.7	15.3	16.1	17.2	18.2	18.9	19.5	20.4	21.0	21.7	22.9
2	1×	49.7	8.4	4.4	3.3	2.8	2.6	2.6	2.6	2.6	2.6	2.7	2.7	2.8	2.9	3.0	3.2	3.2	3.4	3.5	3.5
	10×	48.6	9.5	6.0	5.2	5.0	5.2	5.2	5.3	5.4	5.8	6.4	6.6	7.0	7.1	7.5	8.0	8.3	8.6	9.0	9.2
	100×	51.8	14.7	11.8	11.5	11.5	11.9	13.2	14.0	14.3	15.3	16.2	16.9	18.4	19.2	19.8	21.0	22.0	22.8	23.2	24.3
2.5	1×	53.1	9.1	4.5	3.3	2.8	2.7	2.6	2.5	2.5	2.6	2.7	2.7	2.8	2.8	2.9	3.1	3.2	3.3	3.5	3.6
	10×	53.7	10.5	6.3	5.4	5.1	5.1	5.3	5.4	5.7	6.0	6.3	6.6	6.8	6.9	7.5	8.1	8.3	8.6	8.9	9.2
	100×	57.0	15.6	12.7	11.9	11.8	12.2	13.1	14.3	14.6	15.2	16.3	17.0	18.8	19.2	19.9	21.0	21.9	22.3	23.3	23.7
3	1×	55.5	9.4	4.8	3.4	2.9	2.7	2.6	2.5	2.5	2.5	2.6	2.7	2.7	2.8	2.9	3.0	3.1	3.2	3.4	3.4
	10×	56.0	10.5	6.2	5.3	5.1	5.1	5.1	5.3	5.5	5.7	5.9	6.4	6.4	6.6	7.0	7.8	8.0	8.3	8.6	8.9
	100×	60.3	16.2	12.7	11.7	11.8	12.2	12.6	13.8	14.2	14.6	15.8	16.5	17.6	18.5	19.4	19.8	20.7	21.0	21.8	22.5

Note. — The detection threshold to resolve spatially extended sources with a uniform disk spatial model for a two-year exposure The threshold is calculated for sources of varying energy ranges, spectral indices, and background levels. The sensitivity was calculated against a Sreekumar-like isotropic background and the second column is the factor that the simulated background was scaled by. The remaining columns are varying sizes of the source. The table quotes integral fluxes in the analyzed energy range (1 GeV to 100 GeV or 10 GeV to 100 GeV) in units of 10^{-10} ph cm^{-2} s^{-1}.

Fig. 7: Detection Threshold (cont)

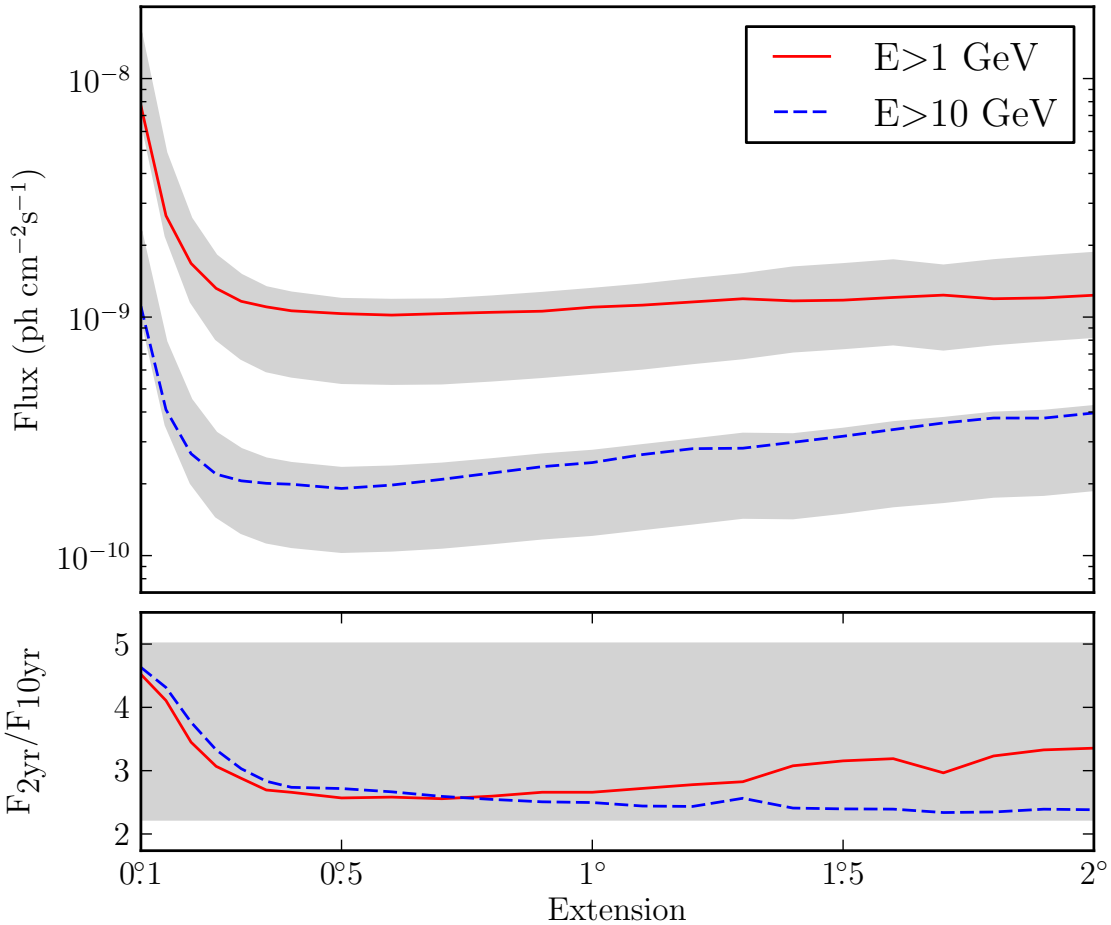

- Compute sensitivty after 10 years.

Fig. 8: Effects of Source Confusion

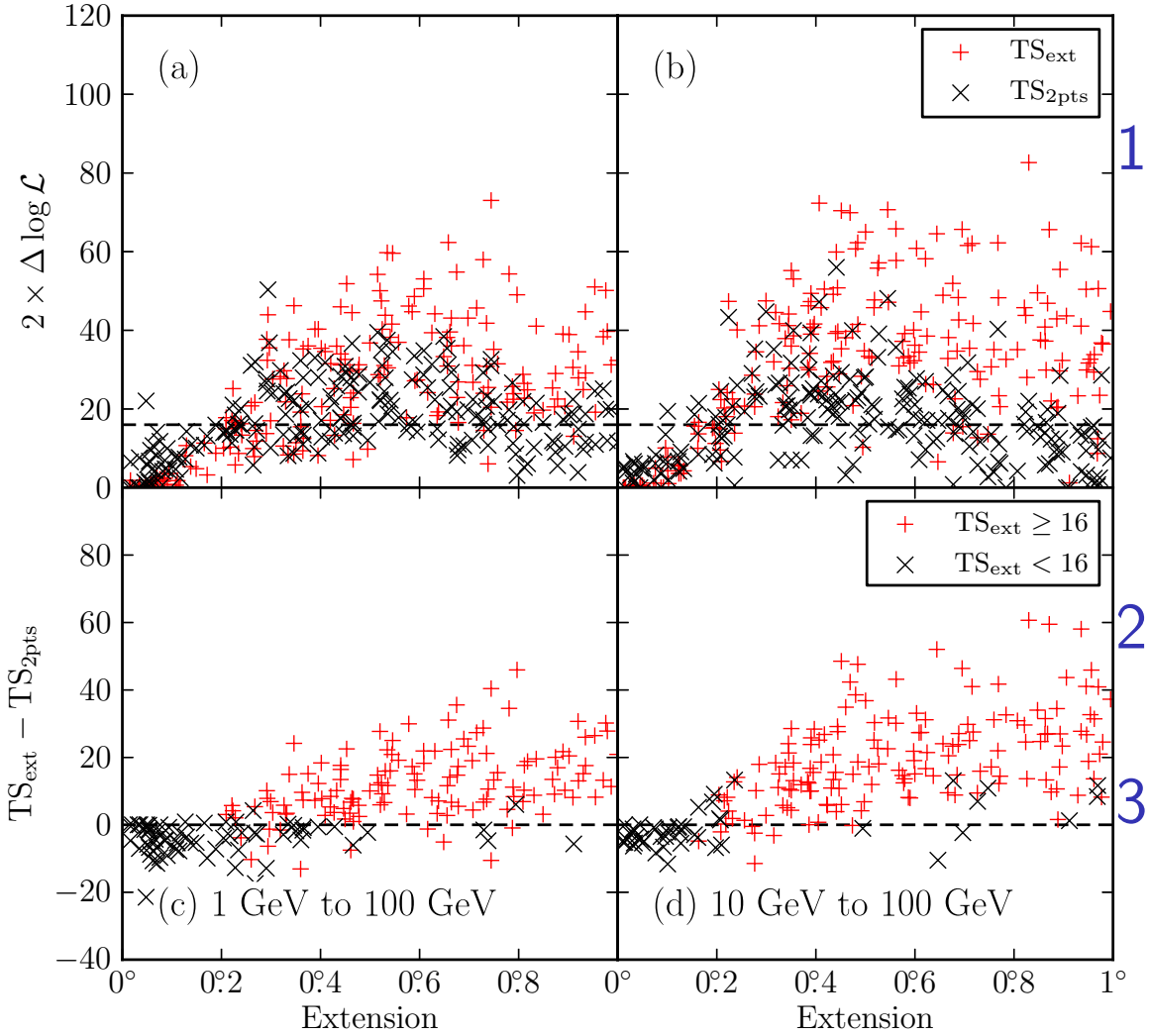

1. Non-nested model comparison

   $\mathrm{TS}_{\mathrm{2pts}} = 2 \log(\mathcal{L}_{\mathrm{2pts}}/\mathcal{L}_{\mathrm{ps}})$

2. Simulate extended sources.
3. Fit as point-like sources.

Fig. 9: Effects of Source Confusion (cont)

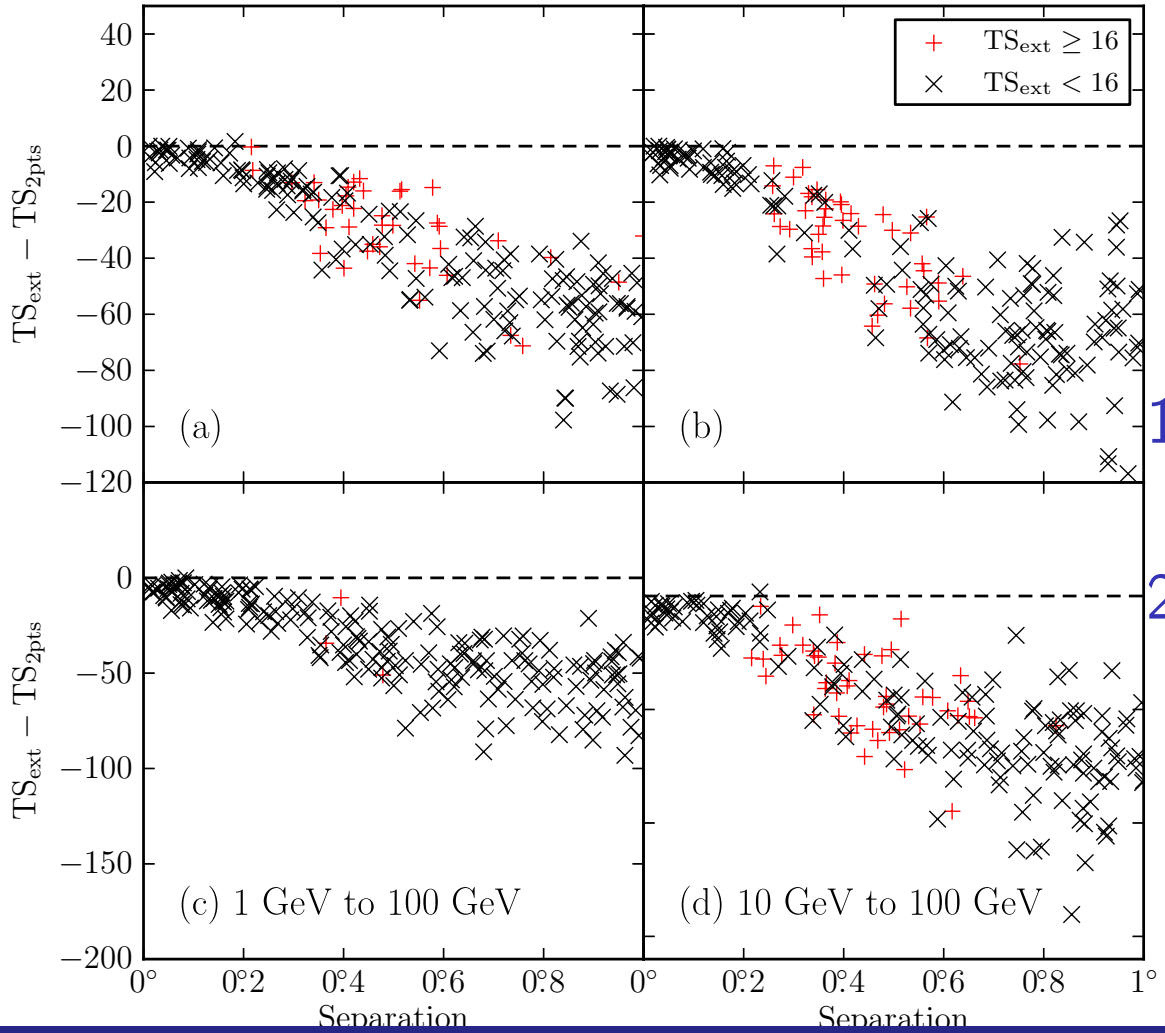

1. Simulate point-like sources.
2. Fit for extension.

Fig. 10: TS_{EXT} for 2LAC AGN

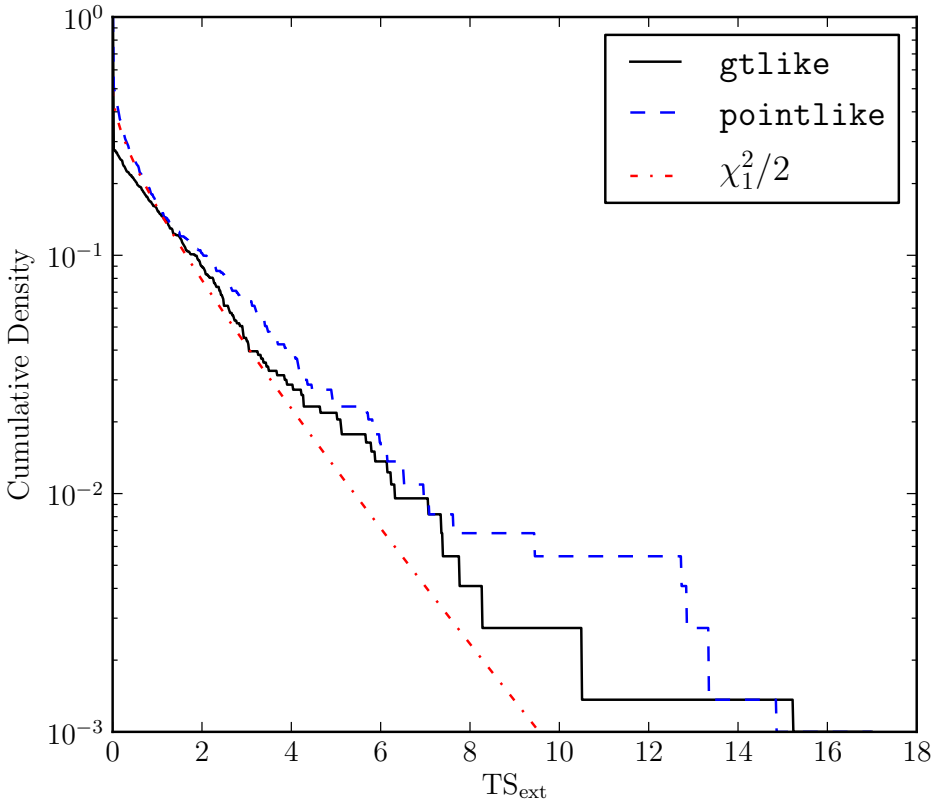

- Use point-like AGN to validate extended source analysis
- Test clean 2LAC AGN for extension
- Don't find AGN to be extended!

Fig. 1 + 11: IC 443

Most significantly extended source

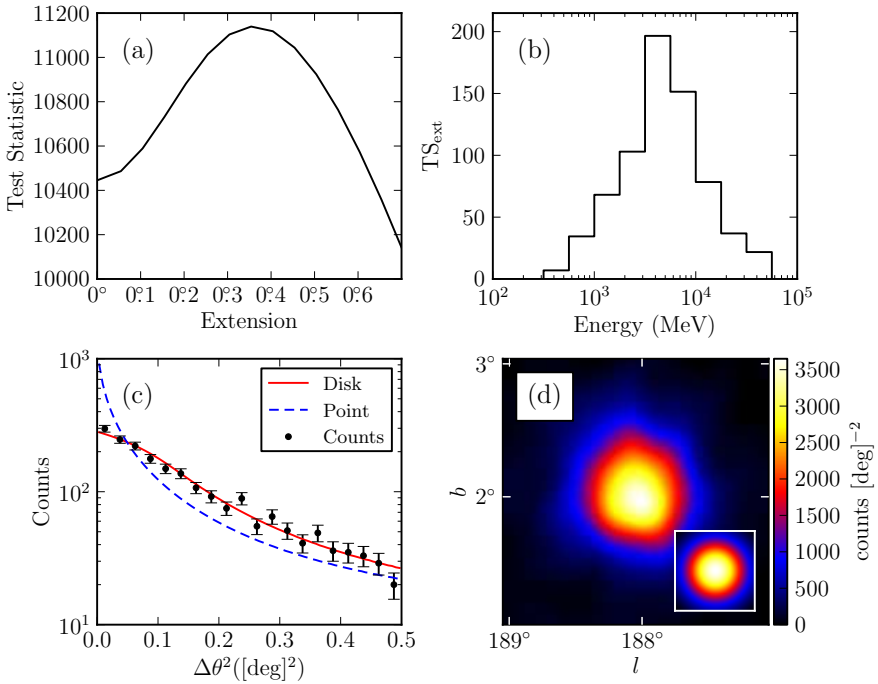

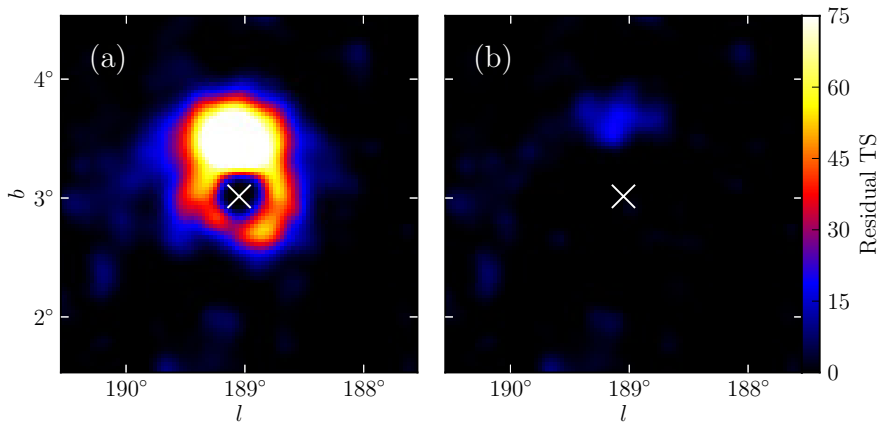

Table 3: extended sources in 2FGL

Table 3. Analysis of the twelve extended sources included in 2FGL

Name	GLON (deg.)	GLAT (deg.)	σ (deg.)	TS	TS_{ext}	Pos Err (deg.)	Flux[(a)]	Index
			E>1 GeV					
SMC	302.59	-44.42	$1.32 \pm 0.15 \pm 0.31$	95.0	52.9	0.14	2.7 ± 0.3	2.48 ± 0.19
LMC	279.26	-32.31	$1.37 \pm 0.04 \pm 0.11$	1127.9	909.9	0.04	13.6 ± 0.6	2.43 ± 0.06
IC443	189.05	3.04	$0.35 \pm 0.01 \pm 0.04$	10692.9	554.4	0.01	62.4 ± 1.1	2.22 ± 0.02
Vela X	263.34	-3.11	0.88					
Centaurus A	309.52	19.42	~ 10					
W28	6.50	-0.27	$0.42 \pm 0.02 \pm 0.05$	1330.8	163.8	0.01	56.5 ± 1.8	2.60 ± 0.03
W30	8.61	-0.20	$0.34 \pm 0.02 \pm 0.02$	464.8	76.0	0.02	29.1 ± 1.5	2.56 ± 0.05
W44	34.69	-0.39	$0.35 \pm 0.02 \pm 0.02$	1917.0	224.8	0.01	71.2 ± 0.5	2.66 ± 0.00
W51C	49.12	-0.45	$0.27 \pm 0.02 \pm 0.04$	1823.4	118.9	0.01	37.2 ± 1.3	2.34 ± 0.03
Cygnus Loop	74.21	-8.48	$1.71 \pm 0.05 \pm 0.06$	357.9	246.0	0.06	11.4 ± 0.7	2.50 ± 0.10
			E>10 GeV					
MSH15−52	320.39	-1.22	$0.21 \pm 0.04 \pm 0.04$	76.3	6.6	0.03	0.6 ± 0.1	2.20 ± 0.22
HESS J1825−137	17.57	-0.45	$0.65 \pm 0.04 \pm 0.02$	82.9	44.9	0.05	1.8 ± 0.8	1.83 ± 0.73

[(a)]Integral Flux in units of 10^{-9} ph cm^{-2} s^{-1} and integrated in the fit energy range (either 1 GeV to 100 GeV or 10 GeV to 100 GeV).

Note. — All sources were fit using a spatial model assuming a uniform radially symmetric intensity distribution. GLON and GLAT are Galactic longitude and latitude of the best fit extended source respectively. The first error on σ is statistical and the second is systematic (see Section 8). The errors on the integral fluxes and the spectral indices are statistical only. Pos Err is the error on the position of the source. Vela X and the Centaurus A Lobes were not fit in our analysis but are include for completeness.

- Test 12 extended 2FGL sources for extension
- Systematic reanalysis using 2 years of data.
- Assume uniform disk
- Extended sources are extended!

Section 9: Extended Source Search

- Run a dedicated search
- Find previously-unresolved extended 2FGL sources
- Search for $E > 1$ GeV and $E > 10$ GeV
- Many difficulties in search, discussed at length in text...
- Publish only good candidates

Fig. 12: Systematics in the plane

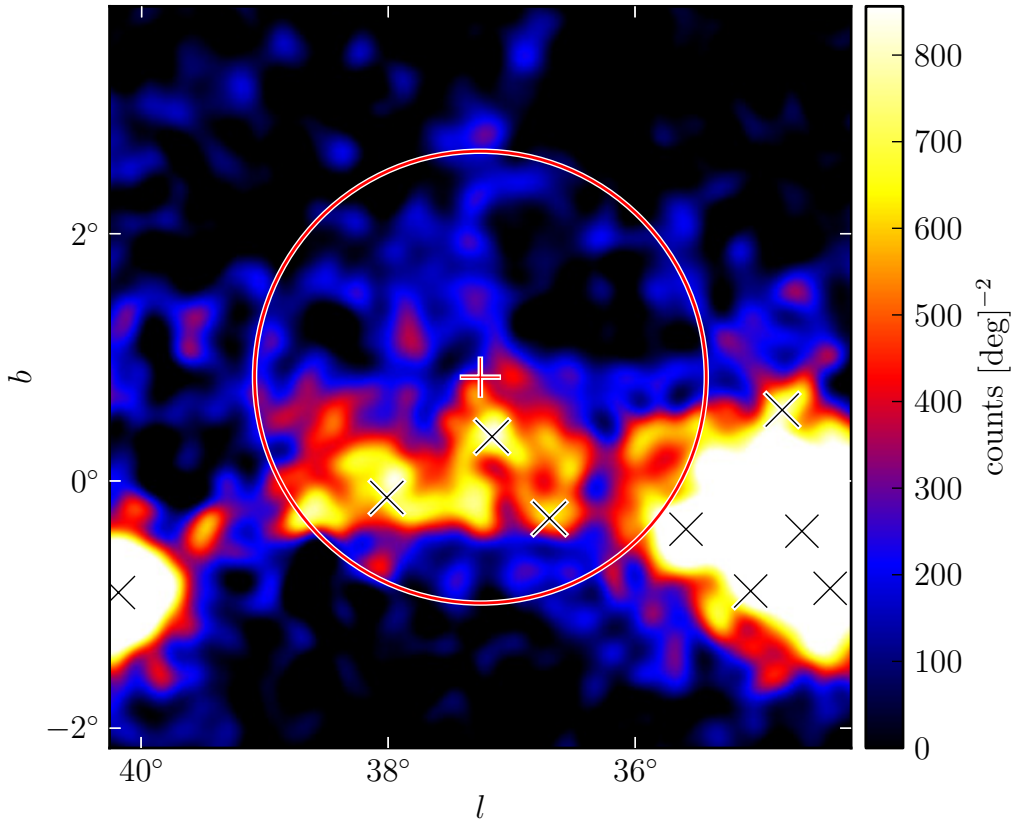

Fig 13: Puppis A

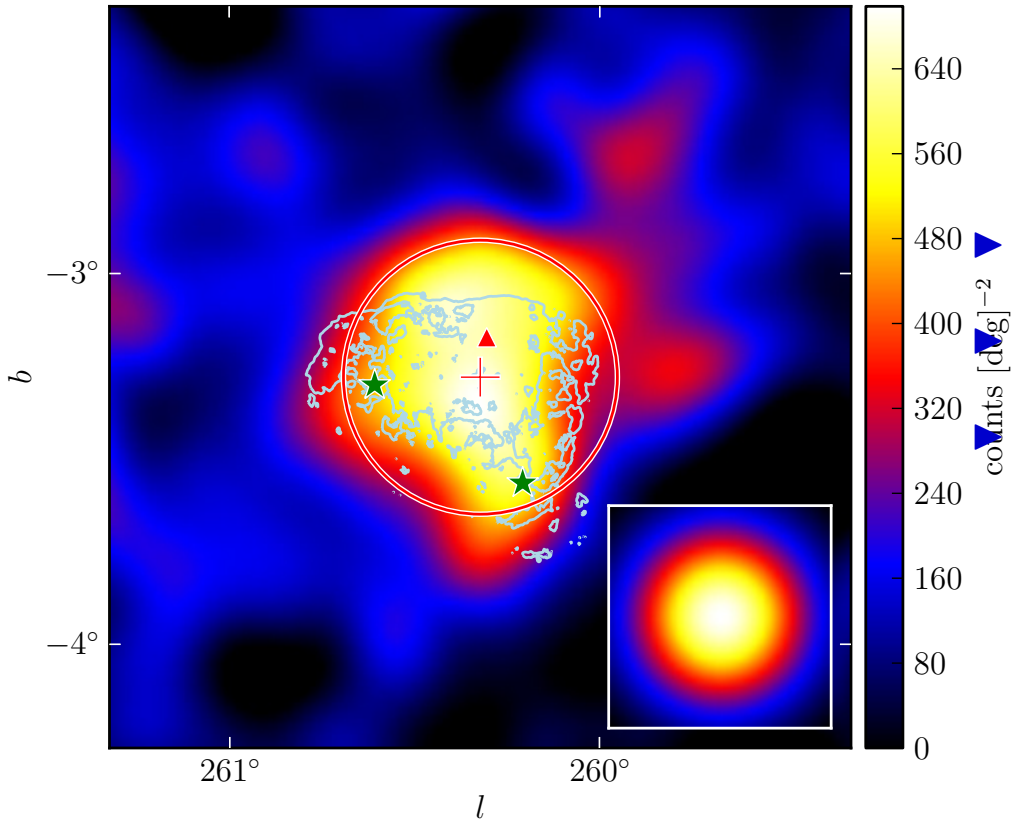

- X-ray contours
- Mid-aged SNR
- Not observed to directly interact with molecular clouds

Fig 22: γ-Cygni

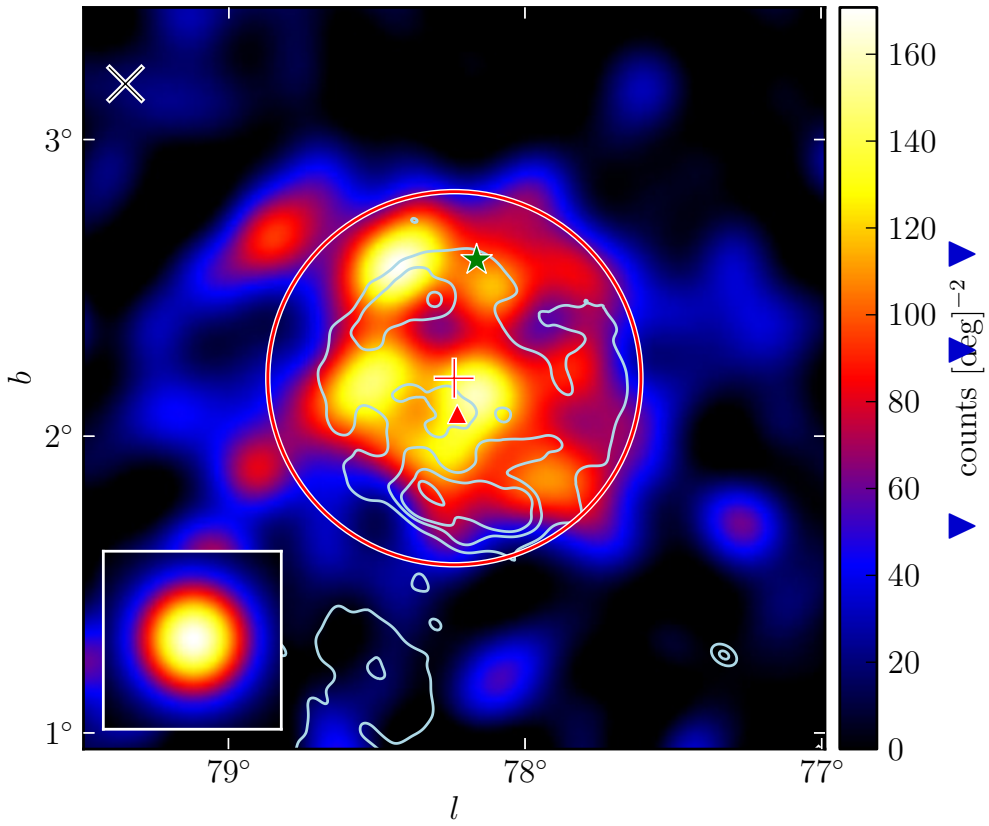

- Radio contours
- SNR interacting with molecular clouds?
- Veritas + Milagro detections

Fig. 14: SED of SNRs

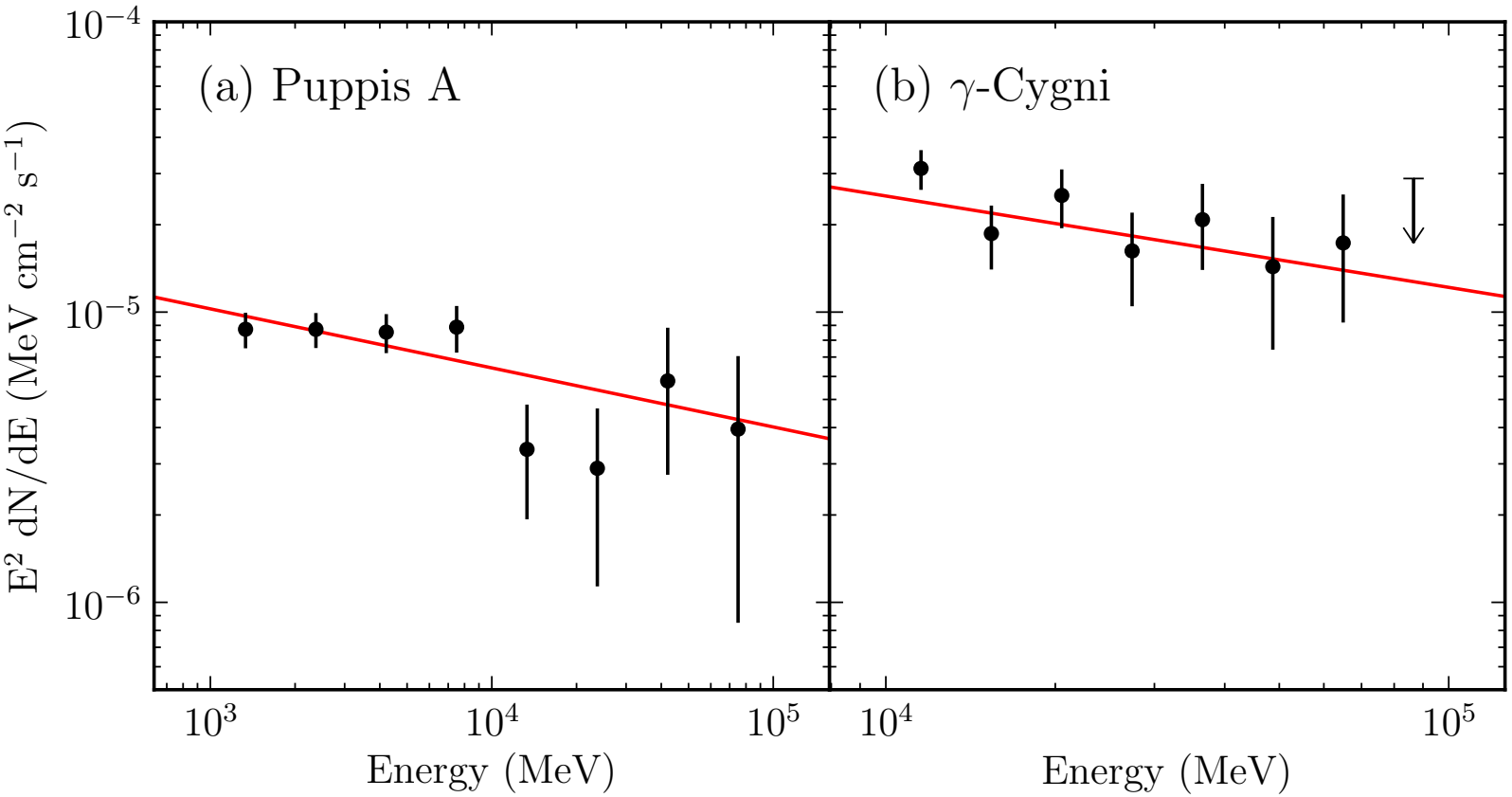

Two Nearby LAT extended sources

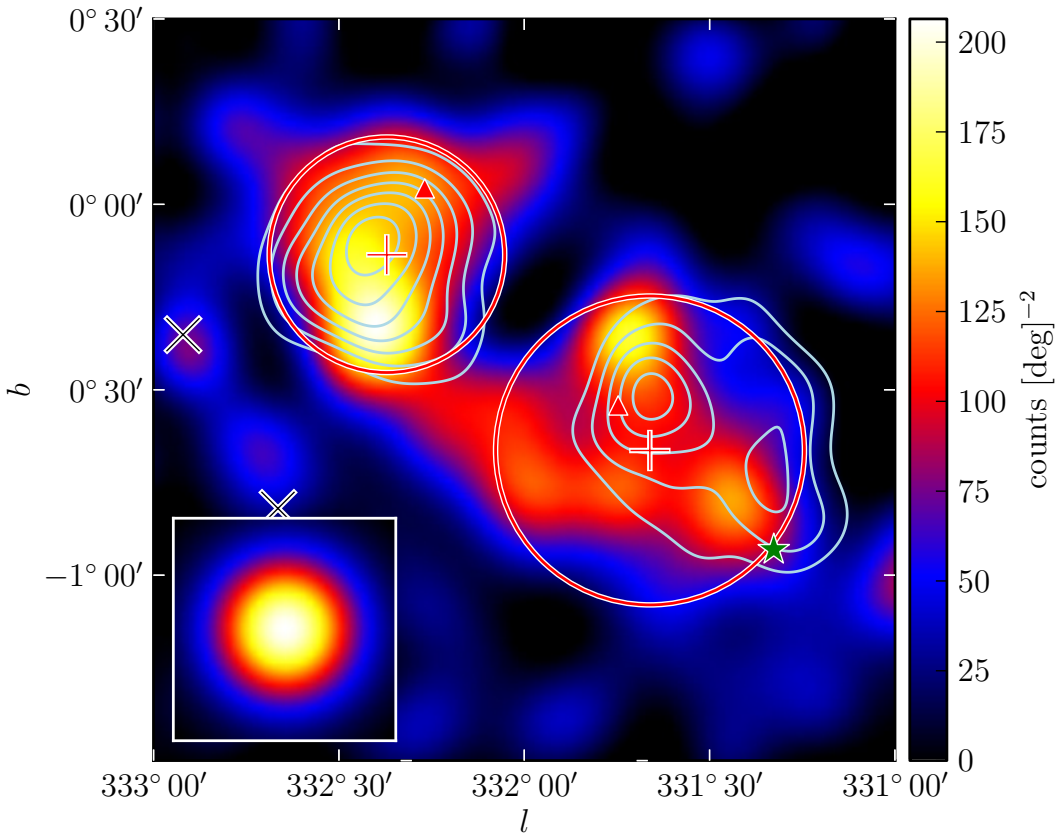

- (left): 2FGL J1615.0−5051
- Coincident with HESS J1616−508
- + X-ray pulsar PSR J1617−5055 + $\sim 1'$ PWN
- PWN Candidate

- (right): 2FGL J1615.2−5138
- Coincident with HESS J1614−518
- No other compelling multiwavelenth counterpart

Fig 19: 2FGL J1632.4−4753c

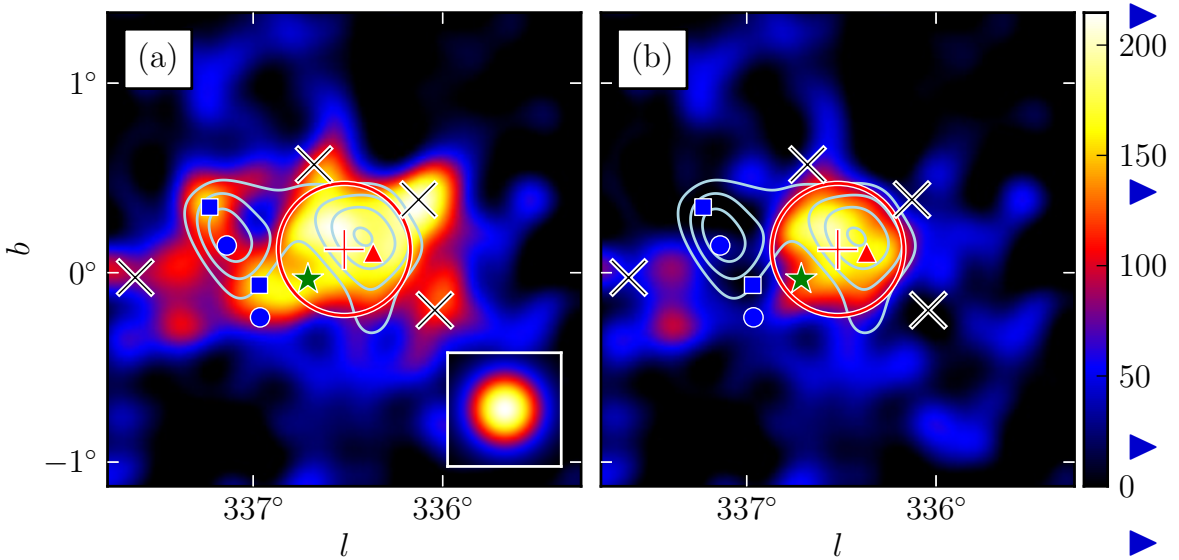

- Coincident with HESS J1632-478
- *XMM-Newton* point-like + extended emission
- (but no pulsations)
- PWN Candidate

Fig 21: 2FGL J1837.3−0700c

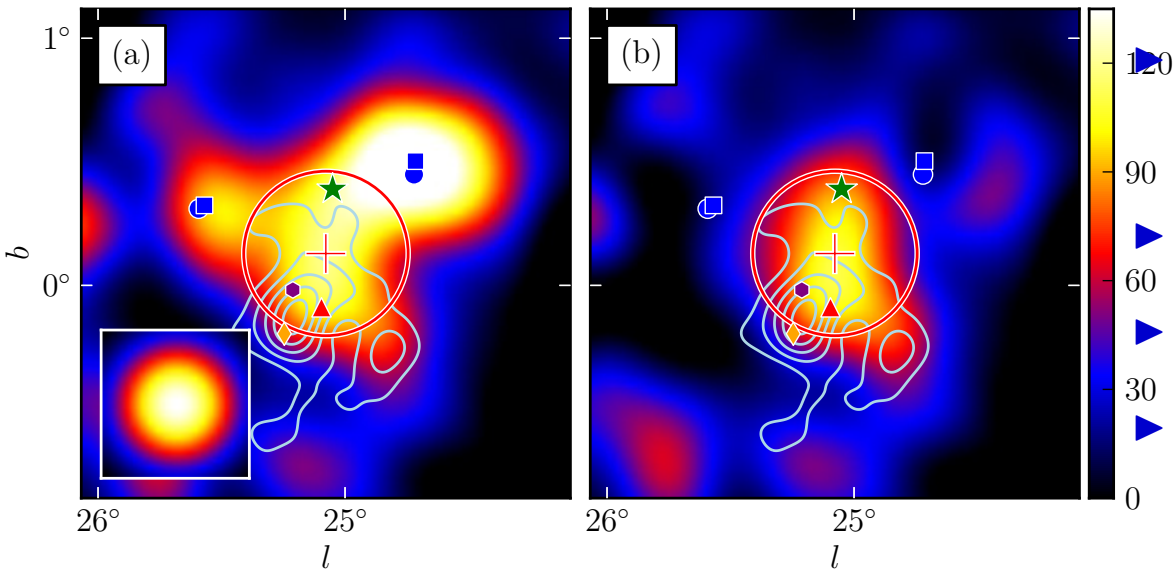

- Coincident with HESS J1837-069
- + X-ray pulsar PSR J1838−0655
- + ∼ 2′ X-ray PWN
- PWN candidate
- Second X-ray PSR + PWN candidate in region (but no pulsations)

Fig. 18: SED of HESS Sources

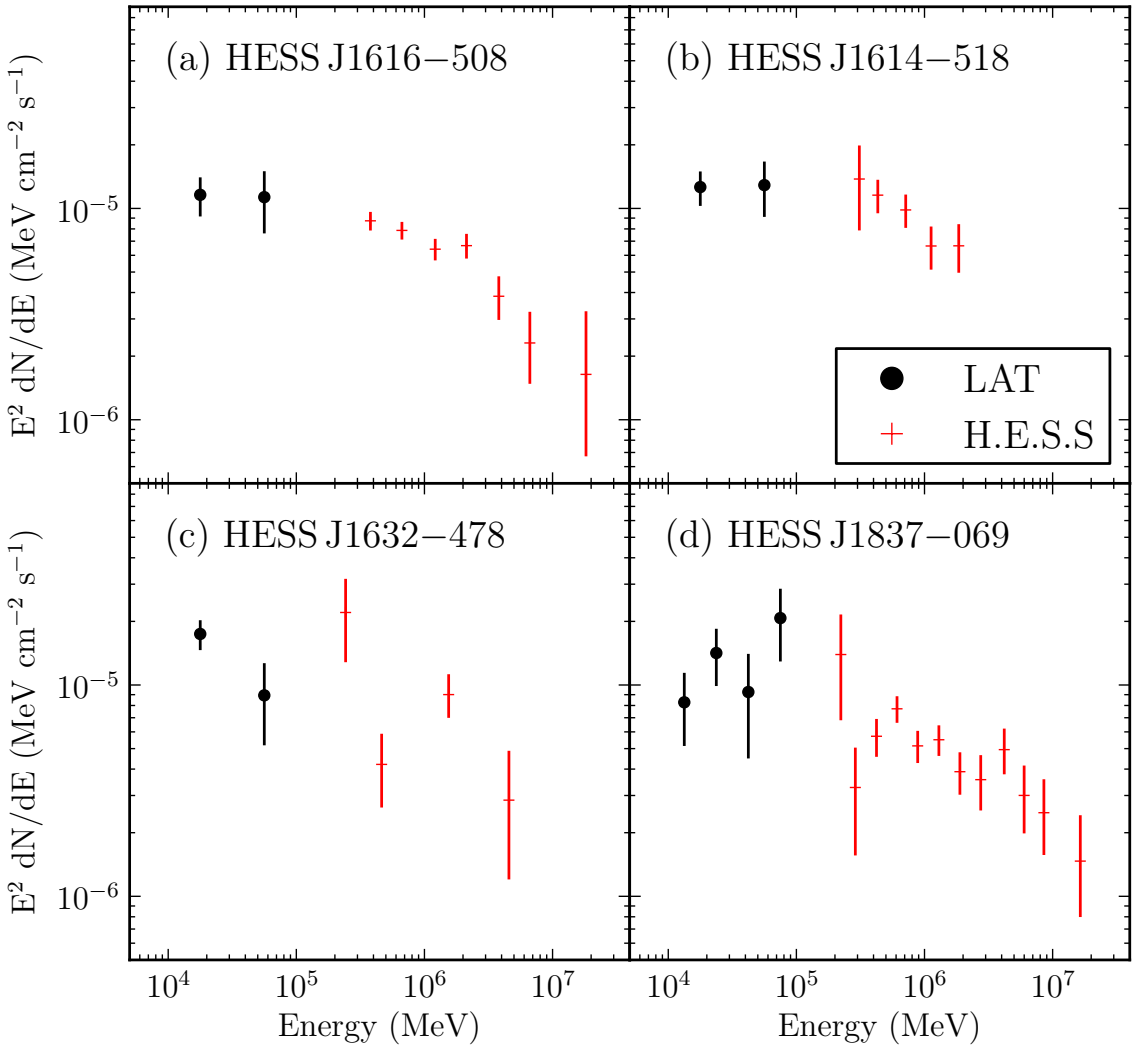

Fig. 20: RX J1713.7−3946

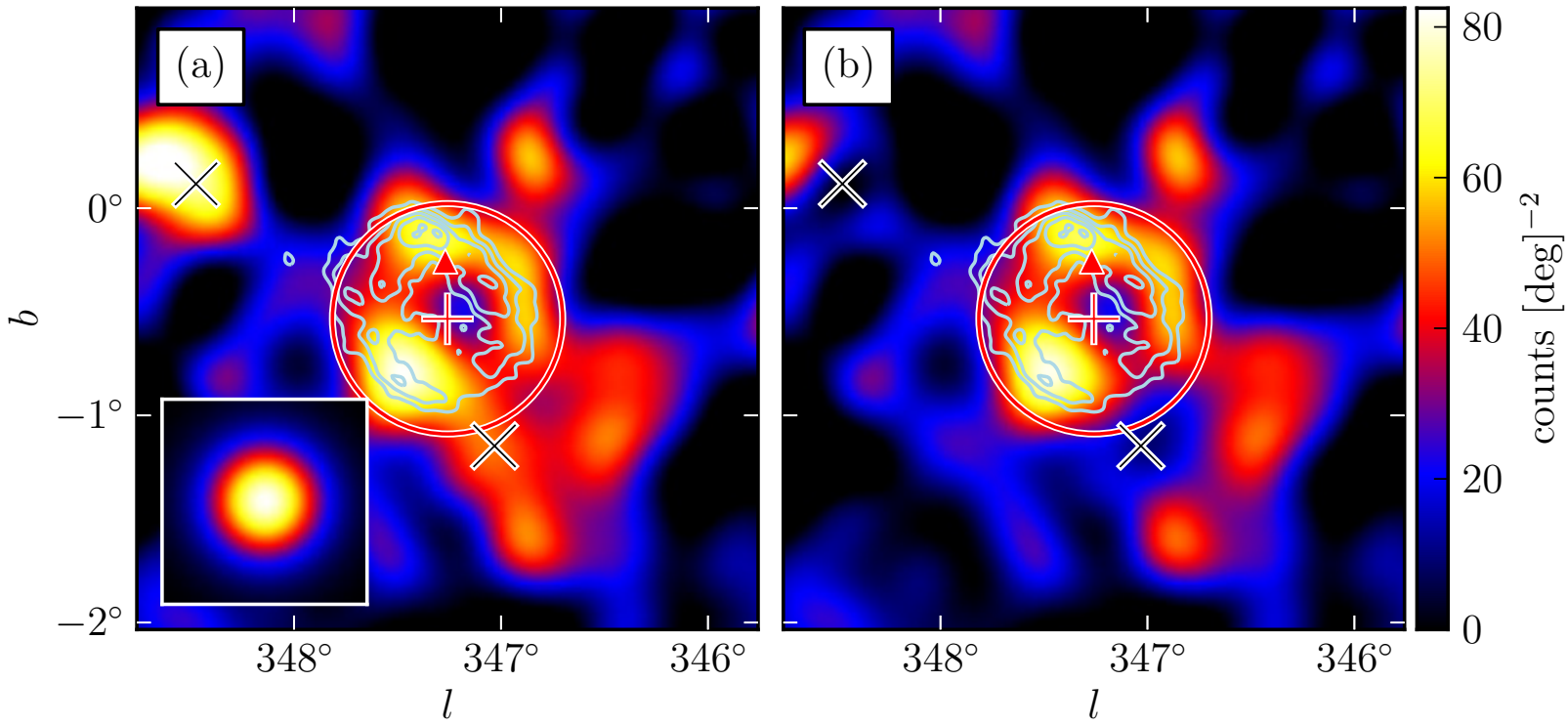

Beauti

GeV Image for E>10 GeV!

Table 4: New extended Sources

Table 4. Extension fit for the nine additional extended sources

Name	GLON (deg.)	GLAT (deg.)	σ (deg.)	TS	TS_{ext}	Pos Err (deg.)	Flux[a]	Index	Counterpart
			E>1 GeV						
2FGL J0823.0−4246	260.32	−3.28	$0.37 \pm 0.03 \pm 0.02$	322.2	48.0	0.02	8.4 ± 0.6	2.21 ± 0.09	Puppis A
2FGL J1627.0−2425c	353.07	16.80	$0.42 \pm 0.05 \pm 0.16$	139.9	32.4	0.04	6.3 ± 0.6	2.50 ± 0.14	Ophiuchus
			E>10 GeV						
2FGL J0851.7−4635	266.31	−1.43	$1.15 \pm 0.08 \pm 0.02$	116.6	86.8	0.07	1.3 ± 0.2	1.74 ± 0.21	Vela Jr.
2FGL J1615.0−5051	332.37	−0.13	$0.32 \pm 0.04 \pm 0.01$	50.4	16.7	0.04	1.0 ± 0.2	2.19 ± 0.28	HESS J1616−508
2FGL J1615.2−5138	331.66	−0.66	$0.42 \pm 0.04 \pm 0.02$	76.1	46.5	0.04	1.1 ± 0.2	1.79 ± 0.26	HESS J1614−518
2FGL J1632.4−4753c	336.52	0.12	$0.35 \pm 0.04 \pm 0.02$	64.4	26.9	0.04	1.4 ± 0.2	2.66 ± 0.30	HESS J1632−478
2FGL J1712.4−3941[b]	347.26	−0.53	$0.56 \pm 0.04 \pm 0.02$	59.4	38.5	0.05	1.2 ± 0.2	1.87 ± 0.22	RX J1713.7−3946
2FGL J1837.3−0700c	25.08	0.13	$0.33 \pm 0.07 \pm 0.05$	47.0	18.5	0.07	1.0 ± 0.2	1.65 ± 0.29	HESS J1837−069
2FGL J2021.5+4026	78.24	2.20	$0.63 \pm 0.05 \pm 0.04$	237.2	128.9	0.05	2.0 ± 0.2	2.42 ± 0.19	γ-Cygni

[a]Integral Flux in units of 10^{-9} ph cm^{-2} s^{-1} and integrated in the fit energy range (either 1 GeV to 100 GeV or 10 GeV to 100 GeV).

[b]The discrepancy in the best fit spectra of 2FGL J1712.4−3941 compared to Abdo et al. (2011e) is due to fitting over a different energy range.

- 6 new extended sources
- + RX J1713-3946 & Vela Jr (not extended in 2FGL)
- + 1 source in Ophiuchus region → diffuse emission

Section 8: Extension Systematics

Test systematics due to not knowing PSF

- Compare best fit extension to MC based PSF
- Use difference as systematic
- Small effect on extension, large effect on statistical significance
- Probably too conservative...

Test systematics due to not knowing PSF

- Break up GALPROP diffuse model into multiple components
- Fit each component locally
- Tests systematics due to imperfect diffuse modeling

Table 5: Dual Localization, alternative PSF, alternative Diffuse

Table 5. Dual localization, alternative PSF, and alternative approach to modeling the diffuse emission

Name	$TS_{\texttt{pointlike}}$	$TS_{\texttt{gtlike}}$	$TS_{alt,diff}$	$TS_{ext\,\texttt{pointlike}}$	$TS_{ext\,\texttt{gtlike}}$	$TS_{ext\,alt,diff}$	σ (deg.)	$\sigma_{alt,diff}$ (deg.)	$\sigma_{alt,psf}$ (deg.)	TS_{2pts}
				E>1 GeV						
2FGL J0823.0−4246	331.9	322.2	356.0	60.0	48.0	56.0	0.37	0.39	0.39	23.0
2FGL J1627.0−2425c	154.8	139.9	105.7	39.4	32.4	24.8	0.42	0.40	0.58	24.5
				E>10 GeV						
2FGL J0851.7−4635	115.2	116.6	123.1	83.9	86.8	89.8	1.15	1.16	1.17	15.5
2FGL J1615.0−5051[(a)]	48.2	50.4	56.6	15.2	16.7	17.8	0.32	0.33	0.32	13.1
2FGL J1615.2−5138	75.0	76.1	83.8	42.9	46.5	54.1	0.42	0.43	0.43	35.1
2FGL J1632.4−4753c	64.5	64.4	66.8	23.0	26.9	25.5	0.35	0.36	0.37	10.9
2FGL J1712.4−3941	59.8	59.4	39.9	38.4	38.5	30.7	0.56	0.55	0.53	2.7
2FGL J1837.3−0700c	44.5	47.0	39.2	17.6	18.5	16.1	0.33	0.32	0.38	10.8
2FGL J2021.5+4026	239.1	237.2	255.8	139.1	128.9	138.0	0.63	0.65	0.59	37.3

[(a)] Using `pointlike`, TS_{ext} for 2FGL J1615.0−5051 was sligthly below 16 when the source was fit in the 10 GeV to 100 GeV energy range. To confirm the extension measure, the extension was refit in `pointlike` using a slightly lower energy. In the 5.6 GeV to 100 GeV energy range, we obtained a consistent extension and TS_{ext} =28.0. In the rest of this paper, we quote the $E > 10$GeV results for consistency with the other sources.

Fig 23: Sky Map of Extended Sources

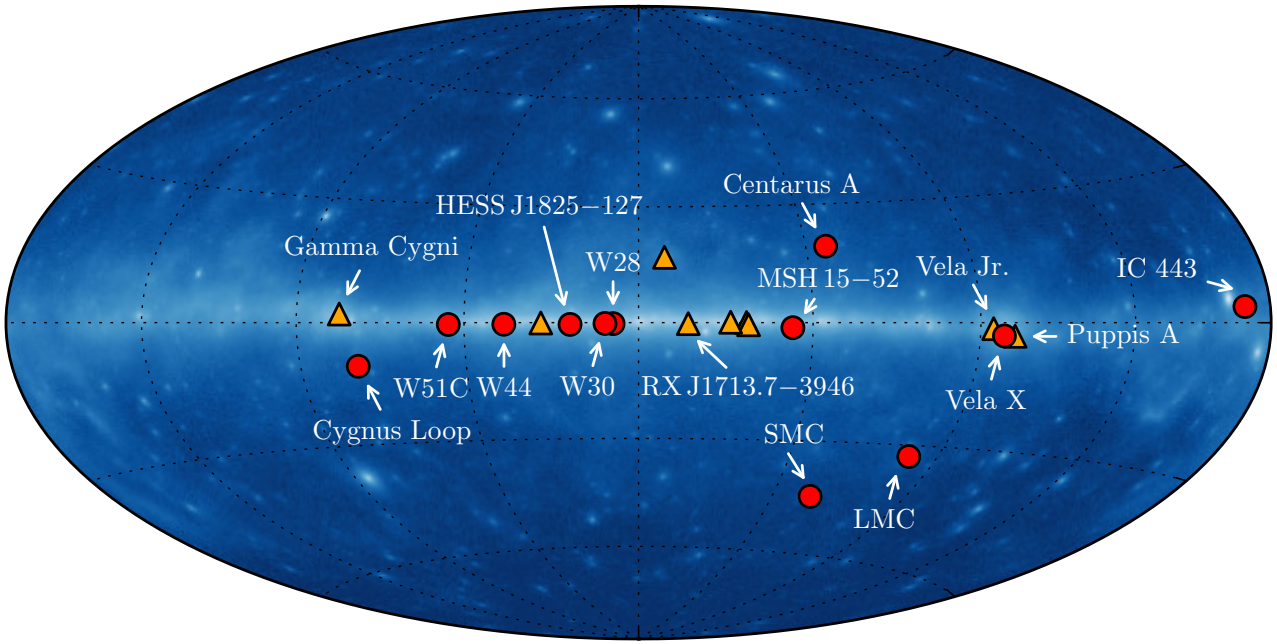

Fig 24: Compare GeV and TeV Sizes

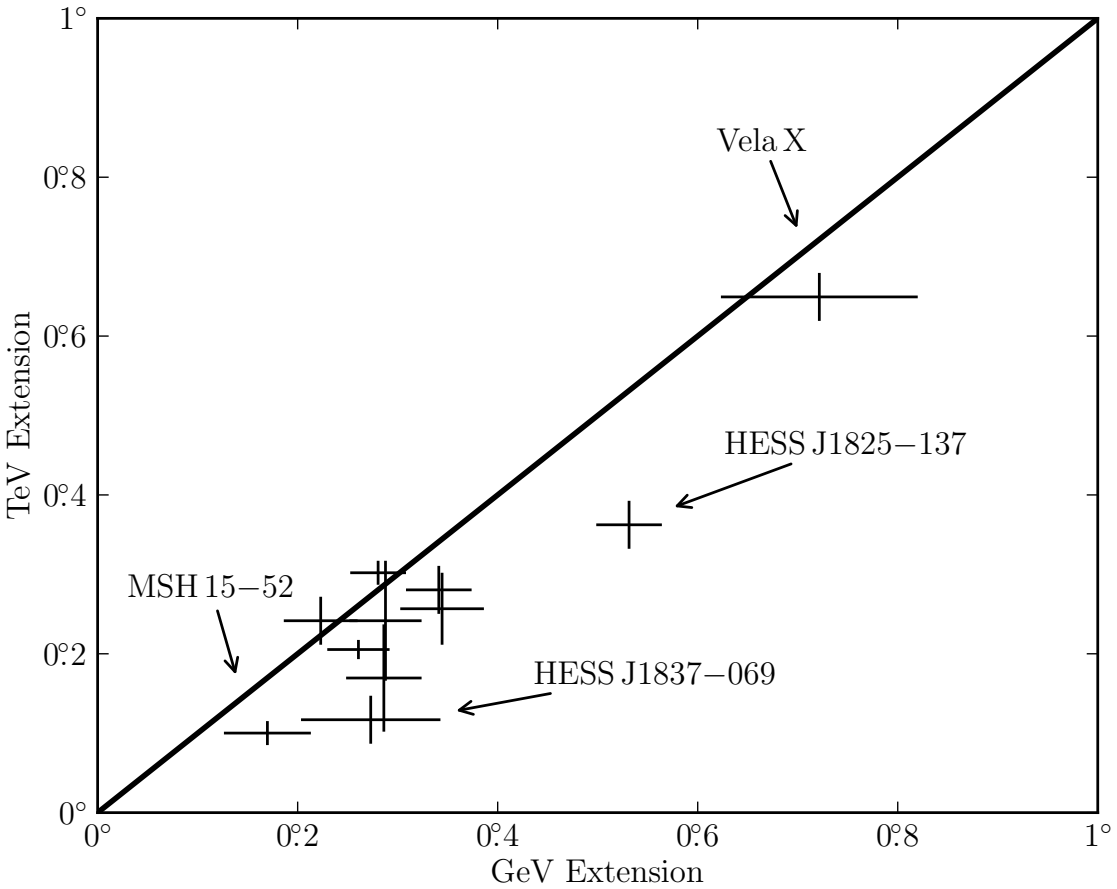

Fig 25: GeV and TeV Sizes (cont)

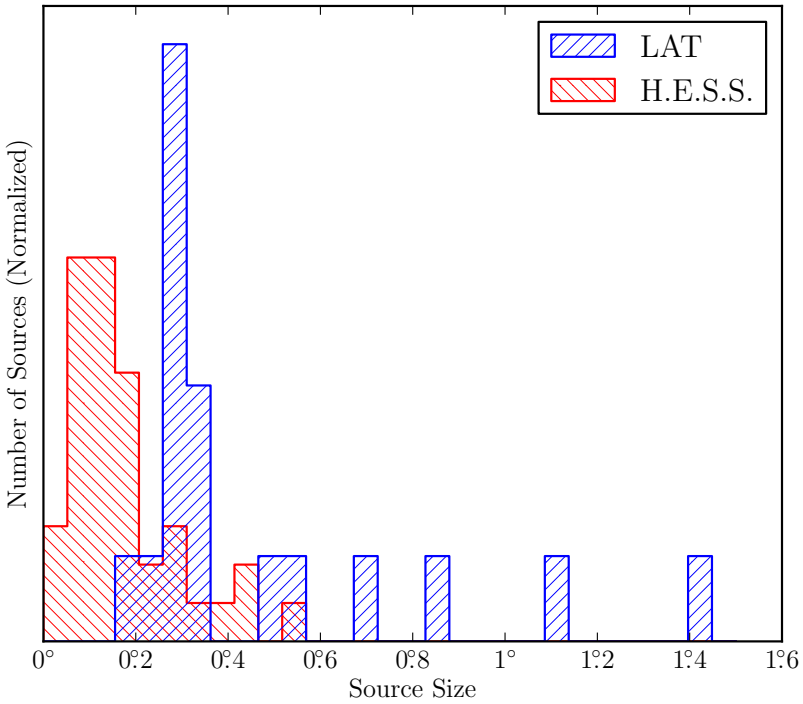

Fig 26: Distribution of Spectral Indices

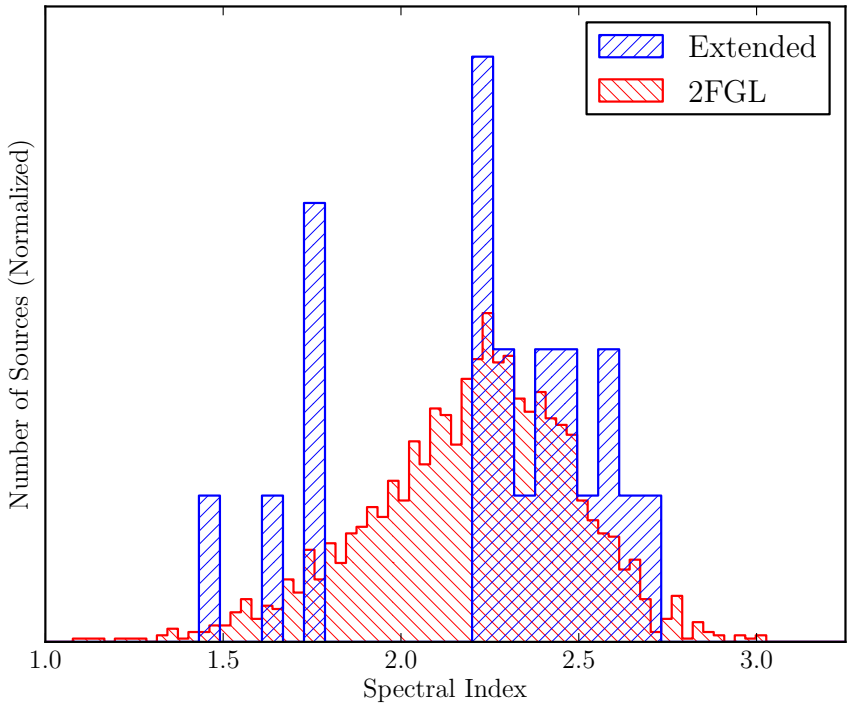

Thank you

See text for more details:

- https://www-glast.stanford.edu/cgi-prot/pub_download?id=662